Modeling and Damping Controller Design for Static Var Compensator

Jawad Faiz
School of Electrical and Computer Engineering,
College of Engineering,
University of Tehran, Iran.
Email: jfaiz@ut.ac.ir

Ghazanfar Shahgholian
Department of Electrical Engineering, Najafabad Branch,
Islamic Azad University,
Esfahan, Iran
Email: shahgholian@iaun.ac.ir

***Abstract* – Shunt flexible transmission systems (FACTS) devices are employed to control the damping of electrical power system oscillations. It can operate either in capacitive mode or in inductive mode. Static var compensator (SVC) is utilized for controlling reactive power of power system and regulating the voltage. This paper presents the effects of a SVC-FACTS controller on the electromechanical oscillations damping of single-machine infinite-bus power system. To this end a damping controller is designed using the root locus method. Finally, the role of SVC in improving stability is shown by simulation results and parameters variations on power system responses are discussed.**

Keywords — Shunt FACTS; SVC; Eigenvalues Analysis.

I. INTRODUCTION

A lower performance is expected for power systems by increasing the size and complexity of the networks. The reasons include load flow, low frequency oscillations and voltage quality; all threat the stability of the power system. By controlling the transmitted power factors, it is possible to control the active as well as reactive power flow over the transmission line. Power system performance is enhanced using flexible transmission systems (FACTS) controllers. The major contributions of the FACTS devices include system dynamics, transient stability, increasing power transmission capacity, damping power oscillations, and maintaining network voltage [1].

Several types of FACTS devices have been so far developed. They can be divided into two categories as shown in Fig. 1 [2, 3]. From control point of view, FACTS controllers are divided into four categories: series controllers such as thyristor controlled series capacitor (TCSC) [4], static synchronous series compensator (SSSC) [5], shunt controllers such as static var compensator (SVC) [6, 7], synchronous static compensator (STATCOM) [8], STATCOM with energy-storage system [9], combined series-shunt controllers such as unified power flow controller (UPFC) [10, 11] and finally combined series-series controllers such as interline power controller (IPFC) [12].

A methodology for selecting SVC location based on static voltage stability index has been presented in [13]. It is based on the L-indices of the load buses which include voltage stability information of a normal power flow. A variable reactance model for SVC at steady-state has been studied and implemented in the load flow program using the embedded FACTS devices [14].

Three FACTS devices for voltage sag mitigation including SVC, STATCOM and dynamic voltage restorer (DVR) have been optimally placed using an NGA [15]; the goal of their application is to reduce the overall financial losses in the network due to the voltage sags. SVC can control reactive power in a power system which improves electromechanical oscillations damping. The output of SVC is a variable susceptance.

This paper presents a mathematical model of SVC-FACTS in a SMIB system. A damping controller is designed for the SVC using root locus methods. Appropriate feedback variables that result in a stable closed-loop operation of the system are selected. Finally, influence of shunt FACTS controller scheme is examined by the simulation results.

II. SVC MATHEMATICAL MODEL

The SVC is the most widely used FACTS device in power system regulation. It is a static var generator whose output varies in order to maintain or control the specific parameters of an electric power system. SVC schemes are successfully applied to improve the dynamic performance of power systems. This enhances the transient stability and improves damping.

A typical structure and voltage-current characteristic of SVC has been shown in Fig. 2 and Fig. 3 respectively. The TCR is formed by a reactor in series with a bi-directional thyristor valve that is fired by a phase angle α ranging between 90º and 180º with respect to the capacitor voltage. The SVC provides a system automated impedance matching device.

During the normal operation, SVC controls the total susceptance according to the terminal voltage. In practice, SVC operates as an adjustable reactance compensating both inductive and capacitive elements. It is originally designed to support power systems voltage. The SVC is based on the normal capacitive and inductive elements and control function is arranged by power electronics devices.

In the present paper, an SMIB power system shown in Fig. 4 is considered. An SVC controller is connected to the bus M between the generator terminal (bus T) and the infinite bus (bus B). The reactance of the line from bus T to bus M is X_S and from bus M to bus B is X_R. The impedance of the whole transmission line is $X_H=X_S+X_R$. λ is the ratio of the left part of the line reactance (X_S) and the whole line reactance (X_H) which varies between 0 and 1. It is noted that the resistance of the line is neglected.

978-1-4799-9978-1/151$31.00 ©2015 IEEE

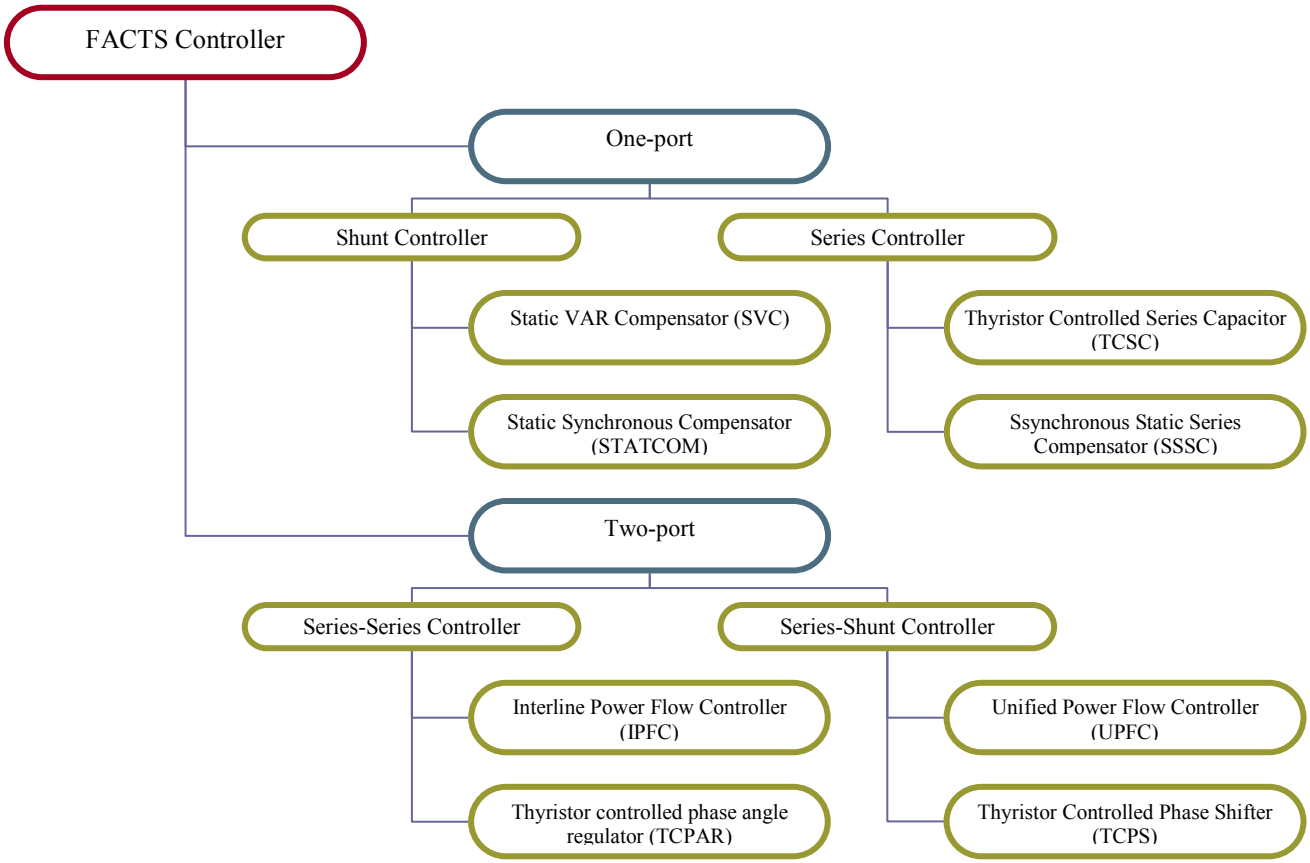

Fig. 1. Overview of compensation devices.

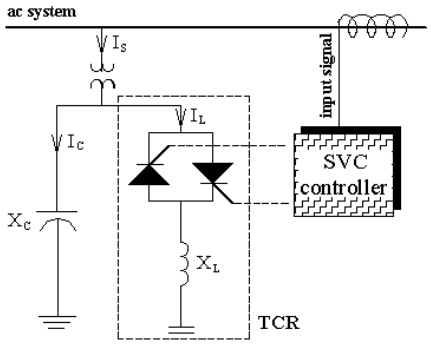

Fig. 2. Typical topology of SVC.

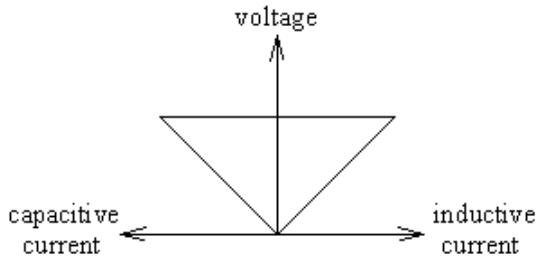

Fig. 3. Voltage-current characteristics of SVC.

The terminal voltage and infinite bus voltage is represented by UT and UB, respectively.

The SVC current in an SMIB power system is as follows:

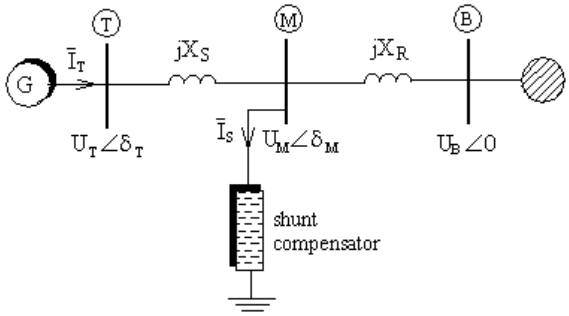

Fig. 4. SMIB power system.

$$\bar{I}_T = \frac{(1 - X_R B_C)\bar{U}_T - \bar{U}_B}{j X_T} \tag{1}$$

where the transfer reactance between the machine internal bus and the infinite bus is: $X_T = X_R + X_S - X_R X_S B_C$. For inductive SVC, $B_C < 0$, and for capacitive SVC $B_C > 0$. For inductive susceptance of SVC, the current is positive. Thus:

$$\bar{I}_S = -j B_C \bar{U}_M \tag{2}$$

The voltage phase angle at bus M is as follows:

$$tg\theta = \frac{d_1 - d_6 B_C}{d_7 - d_3 B_C} \frac{d_2 \sin\delta}{d_4 + d_5 \cos\delta} \tag{3}$$

where coefficients $d_1 \ldots d_7$ depend not only on the system parameters such as quadrature axis reactance (X_q), but also the location of the SVC in the system:

$$\begin{cases} d_1 = X_R + X_S + X_d' \\ d_2 = (X_S + X_q)U_B \\ d_3 = (X_S + X_q)X_R \\ d_4 = X_R E_q' \\ d_5 = (X_S + X_d')U_B \\ d_6 = (X_S + X_d')X_R \\ d_7 = X_R + X_S + X_q \end{cases} \quad (4)$$

The voltage amplitude at bus M is as follows:

$$U_M = \frac{1}{1-(1-\lambda)\lambda X_H B_E} \times \sqrt{\lambda^2 U_B^2 + (1-\lambda)^2 U_T^2 + 2\lambda(1-\lambda)U_T U_B \cos\delta_T} \quad (5)$$

The delivered electrical power P_E is as follows:

$$P_E = \frac{U_B U_T}{X_H} \frac{1}{1-\lambda(1-\lambda)X_H B_C} \sin\delta_T \quad (6)$$

The electrical output power of the generator is:

$$P_E = \frac{E_q' U_B}{X_D} \sin\delta - \frac{U_B^2 (X_q - X_d')}{2 X_D X_Q} \sin 2\delta \quad (7)$$

where

$$X_Q = X_T + X_q - X_R X_q B_C \quad (8)$$

$$X_D = X_T + X_d' - X_d' X_R B_C \quad (9)$$

SVC is modeled as a controllable reactive susceptance with time delay. The dynamics of the susceptance controller can be written as follows [16]:

$$\frac{d}{dt} B_C = \frac{1}{T_R}(-B_C + K_R u) \quad (10)$$

where K_R and T_R are the gain and time constant of SVC respectively. Input of the SVC regulator is as follows:

$$u = G_W(s)(\underbrace{\omega - \omega_{REF}}_{\Delta\omega}) - G_U(s)(\underbrace{U_M + U_{M-REF}}_{\Delta U_M}) \quad (11)$$

where $G_W(s)$ is the controller in speed loop and $G_U(s)$ is the controller in voltage loop. Fig. 5 shows the block diagram of the linearized system installed with SVC. Constants K_1 and K_2 are derived from the electric torque equation, and K_{UD} and K_{UE} from the SVC bus voltage magnitude.

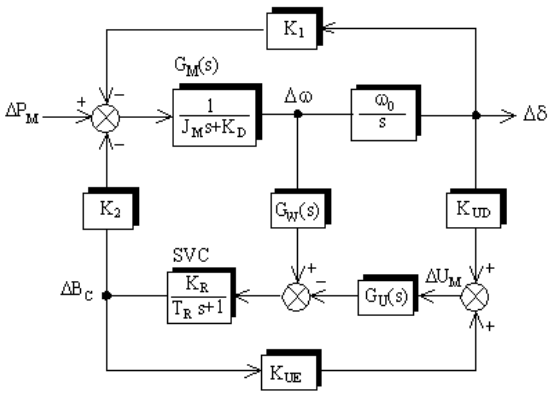

Fig. 5. Block diagram of linearized system with installed SVC.

III. CONTROLLER DESIGN

To design the electromechanical mode damping controllers in the state-space, the non-linear dynamics equations of the power system are linearized around a given operating point. Fig. 6 presents the Simulink model to control the SMIB with the SVC, the key parameters of the model are listed in Table I.

Fig. 7 and Fig. 8 show a root locus of the closed-loop system for investigating the impacts of the feedback gains on the location of the closed-loop poles for normal load. According to these figures, the power system will be stable when K_P changes.

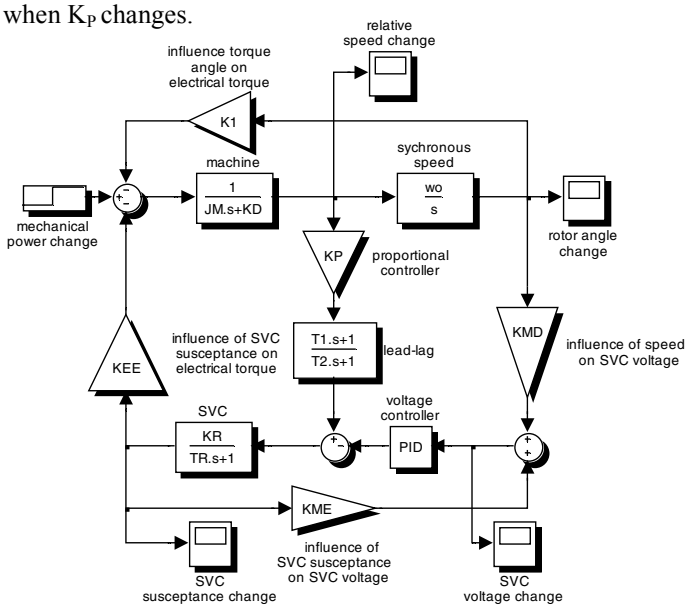

Fig. 6. Block diagram of linearized system installed with SVC.

TABLE I. SYSTEM PARAMETERS

Generator	J_M=6, K_D=4, X_d=1.6, X'$_d$=0.32, X_q=1.55, f=60
Transmission line	X_R=0.2, X_S=0.2
SVC controller	K_R=1.2, T_R=0.2, B_{CO}=0.6
Normal load	P_{EO}=1, Q_{EO}=0.015, U_{TO}=1
Heavy reactive load	P_{EO}=0.8, Q_{EO}=0.4, U_{TO}=1
Importing reactive power	P_{EO}=1, Q_{EO}=-0.2, U_{TO}=1
Controller	K_P=80, T_1=0.5, T_2=0.08, K_{PV}=1, K_{PI}=10

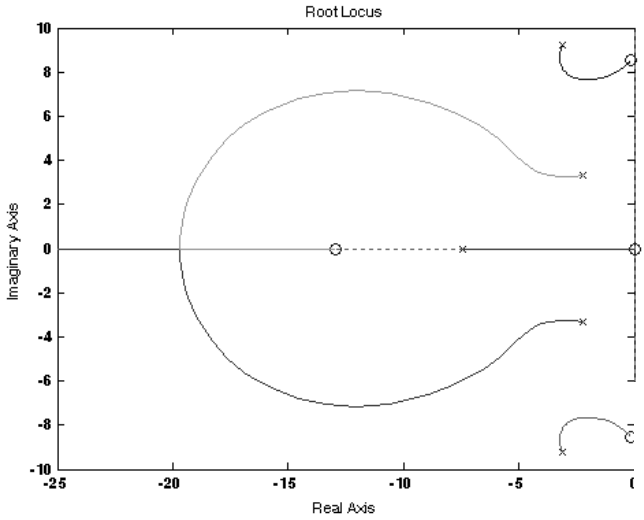

Fig. 7. Locus of roots of power system incremental dynamic for K_P change.

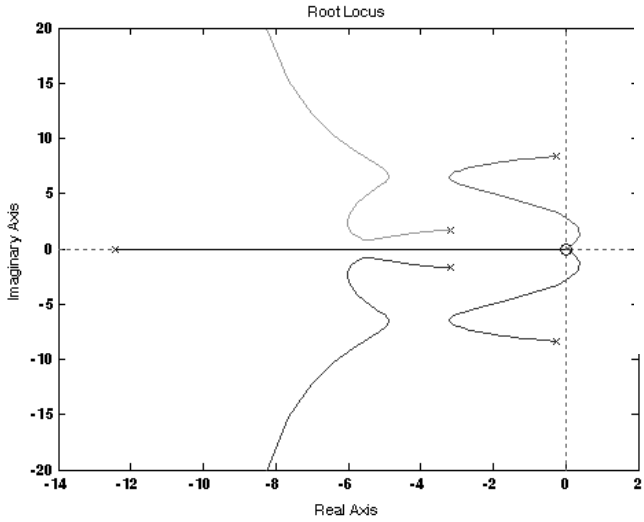

Fig. 8. Locus of roots of power system incremental dynamic for T_1 change.

IV. Simulation Results

The impact of SVC controller on the damping enhancement under system operating changes is investigated in this section. The constant parameters of the linear system for three loading conditions are summarized in Table II. Table III lists the eigen-values of the SMIB power system with the proposed controller. The changes of the rotor angle, voltage bus and susceptance, active and reactive power at the rated load have been shown in Figs. 9, 10 and 11 respectively. The changes of the voltage bus and susceptance for heavy reactive load and importing reactive power have been shown in Figs. 12 and 13 respectively. The simulation results confirm that the system is well stable and damped in all three load conditions

TABLE II. Constants Parameters

Parameters	Normal load	Importing reactive power	Heavy reactive load
K_{DD}	1.4246	1.5595	1.0376
K_{DE}	–0.1163	–0.0731	-–0.1926
K_{QE}	0.1083	0.1860	0.0789
K_{QD}	0.0965	0.0258	0.2279
K_{EE}	0.1241	0.1482	0.0680
K_{ME}	0.1984	0.2107	0.1694
K_{MD}	0.1221	–0.1399	–0.7280
K_1	1.1227	0.2107	0.9654

TABLE III. System Eigen-values with the Proposed Controller

Load condition	No controller	With controller
Normal load	–0.3333±j5.7857	–3.1827±j8.6090 (η=0.3468) –4.1722±j3.3501 -4.6470
Heavy reactive load	–0.3333±j8.6089	–1.6166±j7.7381 (η=0.2045) –3.7332±j1.0187 -8.4832
Importing reactive power	–0.3333±j3.3882	–3.9346±j 9.2342 (η=0.3920) –3.5242±j3.9208 -4.5130

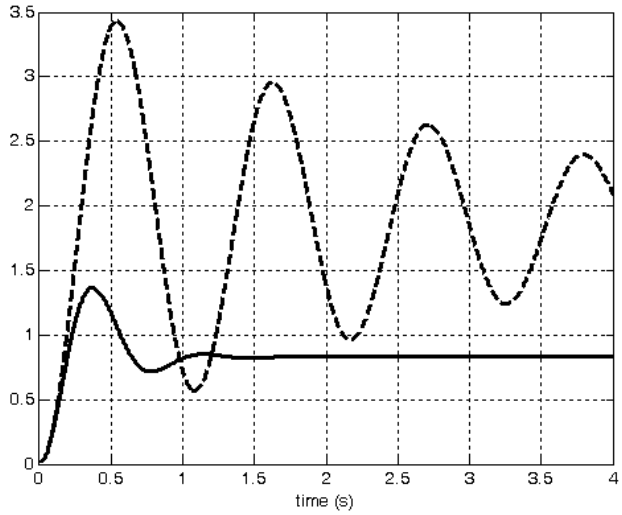

Fig. 9. Rotor angle deviation at rated load with (solid) and without (dot) controller.

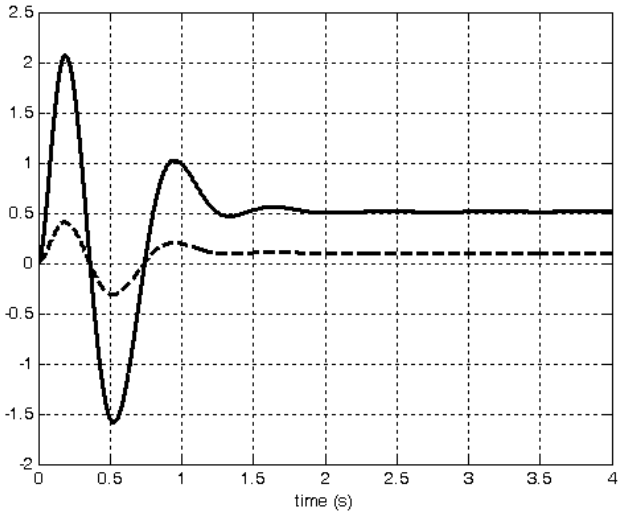

Fig. 10. Susceptance (solid) and bus voltage (dot) deviation at rate load.

V. Conclusion

In this paper the impact of SVC controller in damping oscillatory was analyzed. The dynamic behavior of power system was presented by a developed linearized block diagram of a SMIB power system with a SVC controller.

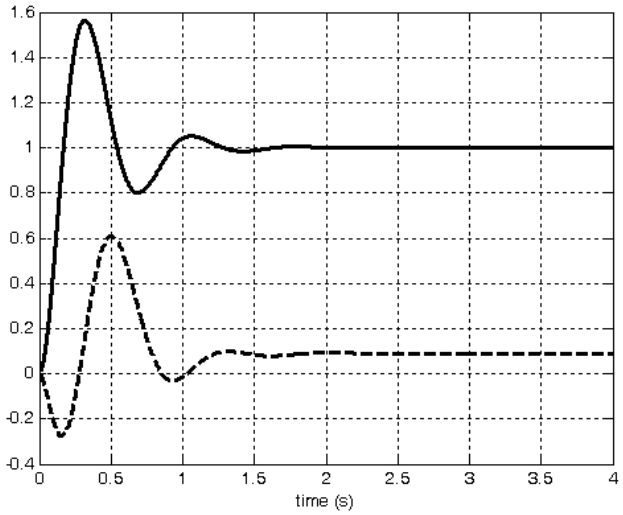

Fig. 11. Active (solid) and reactive (dot) power deviation at rated load.

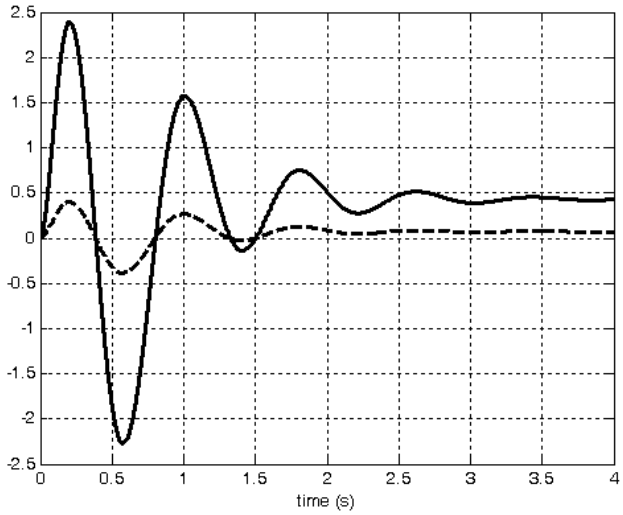

Fig. 12. Susceptance (solid) and bus voltage (dot) deviation at heavy reactive power.

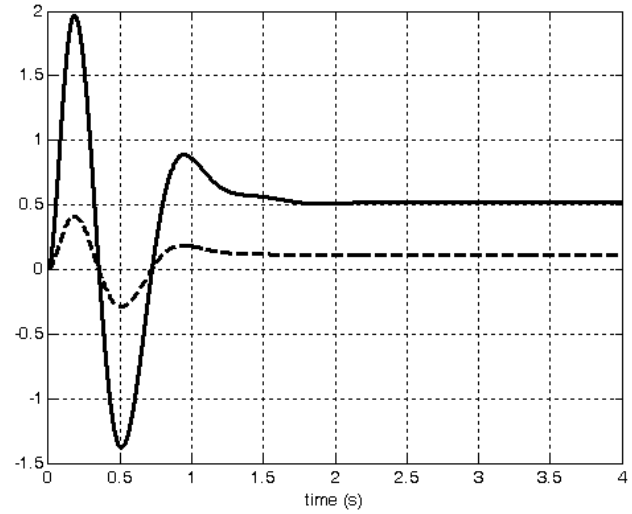

Fig. 13. Susceptance (solid) and bus voltage (dot) deviation at importing reactive power.

The simulation results indicated that the lead-lag controller can improve the stability of power system even when the operating conditions change

References

[1] Y. Yu, C. Jianye, H. Yingduo, "STATCOM modeling and analysis in damping power system oscillation", *IEEE/IECEC*, Vol. 2, pp. 756-762, 2000.

[2] G. Shahgholian, J. Faiz, "Static synchronous compensator for improving performance of power system: A review", *Int. Rev. of Elec. Eng.*, Vol. 4, No. 2, pp. Oct. 2010.

[3] K. Li, J. Zhao, C. Zhang, W.J. Lee, "A study on mode-switching control of TCSC based on conditional firing of thyristor", *IEEE Trans. on Pow. Del.*, Vol. 26, No. 2, pp. 1196-1202, April 2011.

[4] S. Panda "Multi-objective evolutionary algorithm for SSSC based controller design", *Elec. Pow. Sys. Res..*, Vol. 79, No. 6, pp. 937-944, 2009.

[5] N. Daratha, B. Das, J. Sharma, "Coordination between OLTC and SVC for voltage regulation in unbalanced distribution system distributed generation", *IEEE Trans. on Pow. Sys.*, Vol. 29, No. 1, pp. 289-299, Jan. 2014.

[6] G. Shahgholian, M. Zinali, A.A. Amini, M. Mahdavian, "Effects of TCSC on damping power system oscillations", IEEE/ICCSN, Vol. V1, pp. 333-337, China, 2011.

[7] N. Karpagam, D. Devaraj, "Application of GA foe SVC-FACTS controller for power system transient stability improvement", *Int. Jou. of Ele. Pow. and Eng. Sys. Eng.*, pp. 105-111, 2009.

[8] A. Yazdani, H. Sepahvand, M.L. Crow, M. Ferdowsi, "Fault detection and mitigation in multilevel converter STATCOMs", I*EEE Trans. on Ind. Elec.*, Vol. 58, No. 4, pp. 1307-1315, April 2011.

[9] R. Kuiava, R.A. Ramos, N.G. Bretas,"Control design of a STATCOM with energy storage system and power quality improvements", *IEEE/ICIT*, pp. 1-6, February 2009.

[10] J. Guo, M.L. Crow, J. Sarangapani, "An improved UPFC control for oscillation damping", *IEEE Trans. on Pow. Sys.*, Vol. 24, No. 1, Feb. 2009.

[11] P. Kasinathan, R. Vairamani, S. Sundramoorthy, "Dynamic performance investigation of dq model with PID controller-based unified power-flow controller", *IET Pow. Elec.*, Vol. 6, No. 5, pp. 843-850, May 2013.

[12] S. Sankar, S. Ramareddy, "Digital simulation of closed loop controlled IPFC using PSPICE", *Int. Jou. of Ele. and Pow. Eng.,* Vol. 2, pp. 99-103, 2008.

[13] D. Thukaram, A. Lomi, "Selection of static VAR compensator location and size for system voltage stability improvement", *Ele. Pow. Sys. Res.*, Vol. 54, pp. 139-150, 2000.

[14] S. R. Najafi, M. Abedi, S. H. Hosseinian, "A Novel approach to optimal allocation of SVC using genetic algorithms and continuation power flow", *IEEE/PECON*, pp. 202-206, Putra Jaya, Nov. 2006.

[15] J.V. Milanovic, Y.Zhang, "Global minimization of financial losses due to voltage sags with FACTS based devices", *IEEE Trans. on Pow. Deli.*, Vol. 25, No. 1, pp. 298-306, Jan. 2010.

[16] M.A. Abido, Y.L. Abdel-Magid, "Coordinated design of a PSS and an SVC-based controller to enhance power system stability", *Elec. Pow. and Ene. Sys.*, No. 25, pp. 695–704, 2003.